Mecánica Computacional Vol. XXI, pp. 755–774
S. R. Idelsohn, V. E. Sonzogni and A. Cardona (Eds.)
Santa Fe–Paraná, Argentina, October 2002

LOCALIZATION PREDICTIONS OF THE MICROPOLAR MICROPLANE THEORY

Guillermo Etse*, Marcela Nieto*, Paul Steinmann†, Alejandro Carosio*

*Centro de Métodos Numéricos y Computacional en Ing.,
Universidad Nacional de Tucumán, CONICET
Avda. Roca 1800, 4000 Tucumán, Argentina
e-mail: getse@herrera.unt.edu.ar, web page: http://www.unt.edu.ar

†Chair for Applied Mechanics
University of Kaiserslautern, Postfach 3049, D-67653, Germany.

Key Words: Micropolar, Microplane, Elastoplasticity, Faillure, Localization.

Abstract.
The micropolar microplane theory by Etse, Nieto and Steinmann (2002) [14] is based on a reformulation of the classical Cosserat theory within the framework of the microplane concept. The resulting constitutive equations and models include available and more precise information of the complex microstructure of engineering materials like concrete and other composites as compared with the classical smeared crack-based material theories. The main aim of this enriched material formulation was the macroscopic modeling and description of anisotropic material response behaviors by means of the well-developed microplane concept applied within a micropolar continuum setting. To derive the micropolar microplane theory a thermodynamically consistent approach was considered whereby the main assumption was the integral relation between the macroscopic and the microscopic free energy as advocated by Carol, Jirasek and Bazant (2001) [10] and Kuhl, Steinmann and Carol (2001) [15]. In this approach the microplane laws were chosen such that the macroscopic Clausius-Duhem inequality was fully satisfied. This theoretical framework was considered to derive both elastic and elastoplastic micropolar microplane models.
After refreshing the most relevant equations of the micropolar microplane theory, this paper focuses on the evaluation of the localization predictions of this constitutive formulation. A comparative analysis with the predictions of the classical micropolar constitutive theory is also included.

1 INTRODUCTION

The experimental evidence in the field of failure behavior of engineering materials in the last years demonstrated that the macroscopic response of real materials does strongly depend on their microstructure and corresponding mechanical features. Therefore, precise failure predictions require constitutive formulations which account for the relevant informations of the microstructure.

As a consequence an increasing tendency to use macroscopic models based on fundamental aspects of the microstructure of the material can be recognized. Without questions, one of the most successful attempts in this sense is the microplane theory pioneered by Bazant & Gambarova (1984) [3], Bazant (1984) [2] and Bazant & Oh (1985) [4] and (1986) [5] on the basis of an original idea by G.I. Taylor (1938) [20].

The most important contribution of the microplane theory comes from its superior capacity to model anisotropic material behaviors. The main assumption of the microplane theory is the relationship between the local or microscopic strain or stress components and the corresponding global or macroscopic tensor. In this sense and presently the cinematic constraint is extensively used instead of the static constraint. So that the strains on each microplane are the resolved components of their macroscopic counterparts.

The potentials of the microplane theory for describing non linear response behaviors of engineering cohesive-frictional materials like concrete were extensively demonstrated in the first contributions by Bazant and coauthors related with the microplane theory and, more recently, in the works by Bazant & Prat (1988) [6], Carol, Bazant & Prat (1991 and 1992) [7, 8] and Carol & Bazant (1997) [9], among many others.

The lack of a thermodynamically consistent approach for deriving microplane-based constitutive formulations was advocated by Carol, Jirasek & Bazant (2001) [10] who proposed a method for deriving microplane constitutive formulations within a thermodynamically consistent framework by means of the incorporation of a microscopic free Helmholtz energy on every microplane. This concept was successfully extended for inelastic material behavior such as damage and plasticity by Kuhl, Steinmann & Carol (2001) [15]. However, both this work as well as the previous one by Carol, Jirasek & Bazant (2001) [10] were concerned with classical Boltzmann continua (elastic and inelastic).

Recently Etse, Nieto & Steinmann (2002) citeetse02sc the thermodynamically consistent approach was extended to derive microplane models for micropolar continua in the spirit of the brothers Cosserat (1909) [11]. The motivation was firstly to enrich the microscopic kinematic and strength features of the microplane formulation so as to reproduce particular and more complex behaviors of the internal structure of composite quasi-brittle materials like concrete whereby the presence of aggregates may contribute to the development of microrotations in characteristic planes during load histories beyond the elastic limit. Secondly, the regularization of the post peak response behavior of strain softening materials. In this sense, the incorporation of the micropolar length scale at the microscopic level leads to an intrinsically non local microplane constitutive relation when the

additional degrees of freedom of micropolar continua are activated. This characteristic length accounts for mesh objectivity during FE simulations of softening behaviors.

This work also focouses on the analysis of the localization predictions of the proposed microplane micropolar theory and on the comparison with the corresponding predictions of the classical micropolar theory. Both the first and second localization conditions are considered in the analyses. This analysis demonstrates the regularization capabilities of the microplane micropolar theory as well as the differences with the classical theory.

2 MICROPOLAR COSSERAT THEORY

In this section the relevant equations of the micropolar continuum in the spirit of the brothers Cosserat (1909) [11] are presented. This theory was advocated by several authors during the last decades. One of the most prominent works in this regard was made by Eringen (1968) [13] who presented a detailed analysis of elastic micropolar continua and of their mechanical features. However, the first application of the micropolar continuum in non-linear computational solid mechanics took place at the end of the 1980's in the works by Mühlhaus (1989) [17] and de Borst (1991) [12] who analyzed the potentials of the elastoplastic micropolar constitutive theory to regularize the predictions of post-peak response behaviors of structural systems within the theoretical framework of the smeared-crack approach. In the same line, Steinmann & Willam (1991) [19], Willam & Dietsche (1992) [21], Sluys (1992) [18] and Willam et al. (1995) [22] analyzed the localization indicators and localization properties of nonlinear micropolar continua.

2.1 Equilibrium at Macro Level

The quasi-static form of linear and angular momentum of a micropolar continuum in the 3D domain $\mathcal{B}$ (omitting body forces and body couples for simplicity) reads

$$\begin{aligned} \text{div}\boldsymbol{\sigma}^t &= \mathbf{0} \\ \text{div}\boldsymbol{\mu}^t + \boldsymbol{e} : \boldsymbol{\sigma} &= \mathbf{0} \end{aligned} \tag{1}$$

whereby $\boldsymbol{\mu}$ is a non symmetric second order tensor which represents the couple stresses of the micropolar continuum. The local equilibrium equations of the classical continuum and the corresponding typical symmetric form of the stress tensor $\boldsymbol{\sigma}$ are restored when $\text{div}\boldsymbol{\mu}^t = \mathbf{0} \rightarrow \boldsymbol{e} : \boldsymbol{\sigma} = \mathbf{0}$. Here $\boldsymbol{e}$ denotes the third order permutation tensor.

2.2 Strain and Curvature at Macro Level

The deformation of the micropolar continuum is a consequence of the simultaneous action of two types of local or micro motions: the classical or translatory ones, represented by the displacement field $\boldsymbol{u}$, and the pointwise rotations characterized by the first order tensor $\boldsymbol{\omega}$. This enriched motion field leads to the following strain measures

$$\begin{aligned} \boldsymbol{\epsilon} &= \nabla_x \boldsymbol{u} - \boldsymbol{\Omega} \\ \boldsymbol{\kappa} &= \nabla_x \boldsymbol{\omega} \end{aligned} \tag{2}$$

with $\boldsymbol{\Omega} = -\boldsymbol{e} \cdot \boldsymbol{\omega}$. Here $\boldsymbol{\epsilon}$ represents the non-symmetric micropolar strain tensor and $\boldsymbol{\kappa}$ is the micro curvature tensor which takes into account the differential changes of the micro rotations in the neighborhood of a point.

The second order strain tensor may finally be decomposed into a symmetric and skew-symmetric contribution $\boldsymbol{\epsilon} = \boldsymbol{\epsilon}^{sym} + \boldsymbol{\epsilon}^{skw}$ with

$$\begin{aligned} \boldsymbol{\epsilon}^{sym} &= \frac{1}{2}[\nabla_x \boldsymbol{u} + \nabla_x^t \boldsymbol{u}] \\ \boldsymbol{\epsilon}^{skw} &= \frac{1}{2}[\nabla_x \boldsymbol{u} - \nabla_x^t \boldsymbol{u}] + \boldsymbol{e} \cdot \boldsymbol{\omega} \end{aligned} \tag{3}$$

3 MICROPLANE THEORY

In the microplane theory the macro-mechanical response behavior of materials is controlled by constitutive equations of characteristic planes or microplanes by means of the static or the kinematic constraint, requiring that either the stresses or the strains on each microplane, respectively, can be derived by projections of their macroscopic counterparts. In this work only the cinematic constraint is considered which is used for the purpose of the present model.

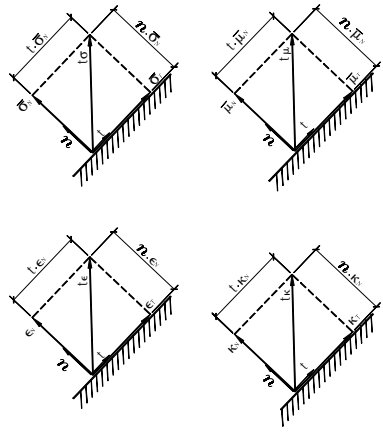

Figure 1: Microplane normal and tangent components of the strain

3.1 Strains and Curvatures at Microplanes

For the case of the kinematic constraint the strain and curvature vectors on each microplane, compare Figure 1, are given by post-multiplication with the microplane normal vector $\boldsymbol{n}$, i.e.

$$\boldsymbol{t}_\epsilon = \boldsymbol{\epsilon} \cdot \boldsymbol{n} = \nabla_n \boldsymbol{u} - \boldsymbol{\omega} \times \boldsymbol{n} \qquad \boldsymbol{t}_\kappa = \boldsymbol{\kappa} \cdot \boldsymbol{n} = \nabla_n \boldsymbol{\omega} \tag{4}$$

The microplane strains and curvatures follow as their normal and tangential components

$$\begin{aligned} \boldsymbol{\epsilon}_N &= \epsilon_N \boldsymbol{n} \qquad \boldsymbol{\kappa}_T = \boldsymbol{t}_\kappa - \boldsymbol{\kappa}_N \\ \boldsymbol{\kappa}_N &= \kappa_N \boldsymbol{n} \qquad \boldsymbol{\epsilon}_T = \boldsymbol{t}_\epsilon - \boldsymbol{\epsilon}_N \end{aligned} \tag{5}$$

These equations are valid both for the symmetric as well as for the skew-symmetric parts of the strain and curvature measures. Taking into account the following properties

$$\begin{aligned} \boldsymbol{\epsilon}^{skw} \cdot \boldsymbol{n} &= -\boldsymbol{n} \cdot \boldsymbol{\epsilon}^{skw} \qquad \boldsymbol{\kappa}^{skw} \cdot \boldsymbol{n} = -\boldsymbol{n} \cdot \boldsymbol{\kappa}^{skw} \\ \boldsymbol{\epsilon}^{sym} \cdot \boldsymbol{n} &= \quad \boldsymbol{n} \cdot \boldsymbol{\epsilon}^{sym} \qquad \boldsymbol{\kappa}^{sym} \cdot \boldsymbol{n} = \quad \boldsymbol{n} \cdot \boldsymbol{\kappa}^{sym} \end{aligned} \tag{6}$$

the symmetric and skew-symmetric microplane strain components in the normal and tangential directions of microplanes are then defined by

$$\begin{aligned} \epsilon_N &= \quad \boldsymbol{N} : \boldsymbol{\epsilon}^{sym} = \quad \boldsymbol{N} \quad : \boldsymbol{\epsilon} \\ \boldsymbol{\epsilon}_T^{sym} &= \quad \boldsymbol{T} : \boldsymbol{\epsilon}^{sym} = \quad \boldsymbol{T}^{sym} : \boldsymbol{\epsilon} \\ \boldsymbol{\epsilon}_T^{skw} &= -\boldsymbol{T} : \boldsymbol{\epsilon}^{skw} = -\boldsymbol{T}^{skw} : \boldsymbol{\epsilon} \end{aligned} \tag{7}$$

while the corresponding microplane curvature components in the normal and tangential directions of microplanes are given by

$$\begin{aligned} \kappa_N &= \quad \boldsymbol{N} : \boldsymbol{\kappa}^{sym} = \quad \boldsymbol{N} \quad : \boldsymbol{\kappa} \\ \boldsymbol{\kappa}_T^{sym} &= \quad \boldsymbol{T} : \boldsymbol{\kappa}^{sym} = \quad \boldsymbol{T}^{sym} : \boldsymbol{\kappa} \\ \boldsymbol{\kappa}_T^{skw} &= -\boldsymbol{T} : \boldsymbol{\kappa}^{skw} = -\boldsymbol{T}^{skw} : \boldsymbol{\kappa} \end{aligned} \tag{8}$$

Here, the second and third order projection tensors $\boldsymbol{N}$ and $\boldsymbol{T}$ are defined with $[\mathbf{I}]_{ijkl} = \delta_{ik}\delta_{jl}$ the fourth order identity tensor and $\boldsymbol{n}$ the microplane normal vector as

$$\begin{aligned} \boldsymbol{N} &= \boldsymbol{n} \otimes \boldsymbol{n} \\ \boldsymbol{T} &= \boldsymbol{n} \cdot \mathbf{I} - \boldsymbol{n} \otimes \boldsymbol{n} \otimes \boldsymbol{n} \end{aligned} \tag{9}$$

In addition to the projection tensor $\boldsymbol{T}$ the symmetric and skew-symmetric projection tensors $\boldsymbol{T}^{sym}$ and $\boldsymbol{T}^{skw}$ with $\boldsymbol{T} = \boldsymbol{T}^{sym} + \boldsymbol{T}^{skw}$ are defined as

$$\begin{aligned} \boldsymbol{T}^{sym} &= \boldsymbol{n} \cdot \mathbf{I}^{sym} - \boldsymbol{n} \otimes \boldsymbol{n} \otimes \boldsymbol{n} \\ \boldsymbol{T}^{skw} &= \boldsymbol{n} \cdot \mathbf{I}^{skw} \end{aligned} \tag{10}$$

whereby $[\mathbf{I}^{sym}]_{ijkl} = [\delta_{ik}\delta_{jl} + \delta_{il}\delta_{jk}]/2$ and $[\mathbf{I}^{skw}]_{ijkl} = [\delta_{ik}\delta_{jl} - \delta_{il}\delta_{jk}]/2$ are the symmetric and skew-symmetric parts of the fourth order identity tensor $\mathbf{I} = \mathbf{I}^{sym} + \mathbf{I}^{skw}$.

4 HEMISPHERICAL INTEGRATIONS

The integration properties of the microplane normal vector $\boldsymbol{n}$ are documented e.g. in the works of by Bazant & Oh (1986) [5] and Lubarda & Krajcinovic (1993) [16] and are applied to perform analytical integrations over the hemisphere Ω

$$\begin{aligned} \int_\Omega d\Omega &= 2\pi \\ \int_\Omega \boldsymbol{n} \otimes \boldsymbol{n} \; d\Omega &= \frac{2\pi}{3} \boldsymbol{I} \\ \int_\Omega \boldsymbol{n} \otimes \boldsymbol{n} \otimes \boldsymbol{n} \otimes \boldsymbol{n} \; d\Omega &= \frac{2\pi}{3} \left[\mathbf{I}_{vol} + \frac{2}{5} \mathbf{I}^{sym}_{dev} \right] \end{aligned} \tag{11}$$

with $[\boldsymbol{I}]_{ij} = \delta_{ij}$ the second order identity tensor and the volumetric and symmetric deviatoric fourth order projection tensors defined as

$$\mathbf{I}_{vol} = \frac{1}{3} \boldsymbol{I} \otimes \boldsymbol{I} \qquad \mathbf{I}^{sym}_{dev} = \mathbf{I}^{sym} - \mathbf{I}_{vol} \tag{12}$$

For later use the relevant products of the projection tensors $\boldsymbol{T}$ and $\boldsymbol{N}$ are given as

$$\left[\boldsymbol{T}^T \cdot \boldsymbol{T}\right]_{ijkl} := T_{aij} T_{akl} = n_i n_k \delta_{jl} - n_i n_j n_k n_l \qquad [\boldsymbol{N} \otimes \boldsymbol{N}]_{ijkl} = n_i n_j n_k n_l \tag{13}$$

and thus integrate over the hemisphere into

$$\frac{3}{2\pi} \int_\Omega \boldsymbol{T}^T \cdot \boldsymbol{T} d\Omega = \mathbf{I}^{skw} + \frac{3}{5} \mathbf{I}^{sym}_{dev} \qquad \frac{3}{2\pi} \int_\Omega \boldsymbol{N} \otimes \boldsymbol{N} d\Omega = \mathbf{I}_{vol} + \frac{2}{5} \mathbf{I}^{sym}_{dev} \tag{14}$$

Accordingly, the relevant products of $\boldsymbol{T}^{sym}$ and $\boldsymbol{T}^{skw}$ are given as

$$\begin{aligned}
\left[[\boldsymbol{T}^{sym}]^T \cdot \boldsymbol{T}^{sym}\right]_{ijkl} &= \frac{1}{4}\left[n_i n_k \delta_{jl} + n_i n_l \delta_{jk} + \delta_{il} n_j n_k + \delta_{ik} n_j n_l\right] - n_i n_j n_k n_l \\
\left[[\boldsymbol{T}^{skw}]^T \cdot \boldsymbol{T}^{skw}\right]_{ijkl} &= \frac{1}{4}\left[n_i n_k \delta_{jl} - n_i n_l \delta_{jk} - \delta_{il} n_j n_k + \delta_{ik} n_j n_l\right] \\
\left[[\boldsymbol{T}^{skw}]^T \cdot \boldsymbol{T}^{sym}\right]_{ijkl} &= \frac{1}{4}\left[n_i n_k \delta_{jl} + n_i n_l \delta_{kj} - \delta_{il} n_j n_k - \delta_{ik} n_j n_l\right]
\end{aligned} \tag{15}$$

and thus integrate over the hemisphere into

$$\begin{aligned}
\frac{3}{2\pi}\int_\Omega [\boldsymbol{T}^{sym}]^T \cdot \boldsymbol{T}^{sym} d\Omega &= \frac{3}{5}\mathbf{I}^{sym}_{dev} \\
\frac{3}{2\pi}\int_\Omega [\boldsymbol{T}^{skw}]^T \cdot \boldsymbol{T}^{skw} d\Omega &= \mathbf{I}^{skw} \\
\frac{3}{2\pi}\int_\Omega [\boldsymbol{T}^{skw}]^T \cdot \boldsymbol{T}^{sym} d\Omega &= \mathbf{O}
\end{aligned} \tag{16}$$

5 THERMODYNAMICALLY CONSISTENT FORMULATIONS

Based on the proposal by Carol, Jirasek and Bazant (2001) [10] and Kuhl, Steinmann and Carol (2001) [15], Etse, Nieto and Steinmann (2002) developed a general formulation for thermodynamically consistent micropolar microplane constitutive laws. In the following we refresh the elastic and elastoplastic forms of the micropolar microplane material formulation.

5.1 Micropolar Microplane Elasticity

In the case of elastic behavior of both the membrane and bending stiffness components the internal variables are zero ($\boldsymbol{q}_u = \boldsymbol{q}_\omega \equiv \mathbf{0}$) and the microscopic free energy reduces to

$$\psi^{mic} = \psi^{mic}_u(\epsilon_N, \boldsymbol{\epsilon}^{sym}_T, \boldsymbol{\epsilon}^{skw}_T) + \psi^{mic}_\omega(\kappa_N, \boldsymbol{\kappa}^{sym}_T, \boldsymbol{\kappa}^{skw}_T) \tag{17}$$

For elasticity the free membrane and bending microscopic free energy can alternatively be expressed in terms of the stored energy

$$\begin{aligned}
\psi^{mic}_u &= W_{N\,u}(\epsilon_N) + W^{sym}_{T\,u}(\boldsymbol{\epsilon}^{sym}_T) + W^{skw}_{T\,u}(\boldsymbol{\epsilon}^{skw}_T) \\
\psi^{mic}_\omega &= W_{N\,\omega}(\kappa_N) + W^{sym}_{T\,\omega}(\boldsymbol{\kappa}^{sym}_T) + W^{skw}_{T\,\omega}(\boldsymbol{\kappa}^{skw}_T)
\end{aligned} \tag{18}$$

whereby for linear elasticity the elastic moduli $E_{N\,u}$, $\mathbf{E}^{sym}_{T\,u}$, $\mathbf{E}^{skw}_{T\,u}$, $E_{N\,\omega}$, $\mathbf{E}^{sym}_{T\,\omega}$ and $\mathbf{E}^{skw}_{T\,\omega}$ were introduced into the microscopic energy functions as

$$W_{N\,u} = \frac{1}{2}\epsilon_N E_{N\,u}\epsilon_N \qquad W^{sym}_{T\,u} = \frac{1}{2}\boldsymbol{\epsilon}^{sym}_T \cdot \mathbf{E}^{sym}_{T\,u} \cdot \boldsymbol{\epsilon}^{sym}_T \qquad W^{skw}_{T\,u} = \frac{1}{2}\boldsymbol{\epsilon}^{skw}_T \cdot \mathbf{E}^{skw}_{T\,u} \cdot \boldsymbol{\epsilon}^{skw}_T \tag{19}$$
$$W_{N\,\omega} = \frac{1}{2}\kappa_N E_{N\,\omega}\kappa_N \qquad W^{sym}_{T\,\omega} = \frac{1}{2}\boldsymbol{\kappa}^{sym}_T \cdot \mathbf{E}^{sym}_{T\,\omega} \cdot \boldsymbol{\kappa}^{sym}_T \qquad W^{skw}_{T\,\omega} = \frac{1}{2}\boldsymbol{\kappa}^{skw}_T \cdot \mathbf{E}^{skw}_{T\,\omega} \cdot \boldsymbol{\kappa}^{skw}_T$$

The definition of the microscopic Clausius-Duhem inequality leads to the microscopic constitutive stresses and couple stresses as thermodynamically conjugate variables to the strain and micro curvature components, respectively

$$\sigma_N = \frac{\partial \psi^{mic}_u}{\partial \epsilon_N} = E_{N\,u}\epsilon_N \qquad \boldsymbol{\sigma}^{sym/skw}_T = \frac{\partial \psi^{mic}_u}{\partial \boldsymbol{\epsilon}^{sym/skw}_T} = \boldsymbol{E}^{sym/skw}_{T\,u} \cdot \boldsymbol{\epsilon}^{sym/skw}_T \tag{20}$$

$$\mu_N = \frac{\partial \psi^{mic}_\omega}{\partial \kappa_N} = E_{N\,\omega}\kappa_N \qquad \boldsymbol{\mu}^{sym/skw}_T = \frac{\partial \psi^{mic}_\omega}{\partial \boldsymbol{\kappa}^{sym/skw}_T} = \boldsymbol{E}^{sym/skw}_{T\,\omega} \cdot \boldsymbol{\kappa}^{sym/skw}_T \tag{21}$$

¿From the macroscopic version of the Clausius-Duhem inequality the macroscopic stress and couple stress tensors follow as functions of the microscopic components

$$\boldsymbol{\sigma}^t = \frac{3}{2\pi}\int_\Omega [\boldsymbol{N} E_{N\,u}\epsilon_N + [\boldsymbol{T}^{sym}]^T \cdot \boldsymbol{E}^{sym}_{T\,u} \cdot \boldsymbol{\epsilon}^{sym}_T - [\boldsymbol{T}^{skw}]^T \cdot \boldsymbol{E}^{skw}_{T\,u} \cdot \boldsymbol{\epsilon}^{skw}_T] d\Omega \tag{22}$$

$$\boldsymbol{\mu}^t = \frac{3}{2\pi}\int_\Omega [\boldsymbol{N} E_{N\,\omega}\kappa_N + [\boldsymbol{T}^{sym}]^T \cdot \boldsymbol{E}^{sym}_{T\,\omega} \cdot \boldsymbol{\kappa}^{sym}_T - [\boldsymbol{T}^{skw}]^T \cdot \boldsymbol{E}^{skw}_{T\,\omega} \cdot \boldsymbol{\kappa}^{skw}_T] d\Omega$$

The last equation can alternatively be rewritten as

$$\begin{aligned} \boldsymbol{\sigma}^t &= \mathbf{E}_u : \boldsymbol{\epsilon} \\ \boldsymbol{\mu}^t &= \mathbf{E}_\omega : \boldsymbol{\kappa} \end{aligned} \tag{23}$$

whereby the macroscopic membrane and bending constitutive moduli are defined as follows

$$\begin{aligned} \mathbf{E}_u &= \frac{3}{2\pi}\int_\Omega [E_{N\,u}\boldsymbol{N}\otimes\boldsymbol{N} + [\boldsymbol{T}^{sym}]^T \cdot \boldsymbol{E}^{sym}_{T\,u} \cdot \boldsymbol{T}^{sym} + [\boldsymbol{T}^{skw}]^T \cdot \boldsymbol{E}^{skw}_{T\,u} \cdot \boldsymbol{T}^{skw}] d\Omega \\ \mathbf{E}_\omega &= \frac{3}{2\pi}\int_\Omega [E_{N\,\omega}\boldsymbol{N}\otimes\boldsymbol{N} + [\boldsymbol{T}^{sym}]^T \cdot \boldsymbol{E}^{sym}_{T\,\omega} \cdot \boldsymbol{T}^{sym} + [\boldsymbol{T}^{skw}]^T \cdot \boldsymbol{E}^{skw}_{T\,\omega} \cdot \boldsymbol{T}^{skw}] d\Omega \end{aligned} \tag{24}$$

Next, under the common assumption of microplane isotropy the tangential strain and curvature vectors and the tangential stress and couple stress vectors remain parallel during the entire load history. Consequently, we consider the following simplification

$$\begin{aligned} \boldsymbol{\epsilon}_T^{sym} \parallel \boldsymbol{\sigma}_T^{sym} &\rightarrow \boldsymbol{E}_{Tu}^{sym} = E_{Tu}^{sym}\, \boldsymbol{I} \\ \boldsymbol{\epsilon}_T^{skw} \parallel \boldsymbol{\sigma}_T^{skw} &\rightarrow \boldsymbol{E}_{Tu}^{skw} = E_{Tu}^{skw}\, \boldsymbol{I} \\ \boldsymbol{\kappa}_T^{sym} \parallel \boldsymbol{\mu}_T^{sym} &\rightarrow \boldsymbol{E}_{T\omega}^{sym} = E_{T\omega}^{sym}\, \boldsymbol{I} \\ \boldsymbol{\kappa}_T^{skw} \parallel \boldsymbol{\mu}_T^{skw} &\rightarrow \boldsymbol{E}_{T\omega}^{skw} = E_{T\omega}^{skw}\, \boldsymbol{I} \end{aligned} \tag{25}$$

Assuming further that the constitutive moduli are independent from the orientation of the microplanes we arrive at

$$\mathbf{E}_u = \frac{3}{2\pi}\left[E_{Nu}\int_\Omega \boldsymbol{N}\otimes\boldsymbol{N}d\Omega + E_{Tu}^{sym}\int_\Omega [\boldsymbol{T}^{sym}]^T\cdot\boldsymbol{T}^{sym}d\Omega + E_{Tu}^{skw}\int_\Omega [\boldsymbol{T}^{skw}]^T\cdot\boldsymbol{T}^{skw}d\Omega\right] \tag{26}$$

$$\mathbf{E}_\omega = \frac{3}{2\pi}\left[E_{N\omega}\int_\Omega \boldsymbol{N}\otimes\boldsymbol{N}d\Omega + E_{T\omega}^{sym}\int_\Omega [\boldsymbol{T}^{sym}]^T\cdot\boldsymbol{T}^{sym}d\Omega + E_{T\omega}^{skw}\int_\Omega [\boldsymbol{T}^{skw}]^T\cdot\boldsymbol{T}^{skw}d\Omega\right]$$

The integration formulae (11) to (17) allow an analytical evaluation of the integrals in eq.(26) to render

$$\begin{aligned} \mathbf{E}_u &= \left[\frac{3}{5}E_{Nu} - \frac{3}{5}E_{Tu}^{sym}\right]\boldsymbol{I}_{vol} + \left[\frac{2}{5}E_{Nu} + \frac{3}{5}E_{Tu}^{sym}\right]\mathbf{I}^{sym} + E_{Tu}^{skw}\,\mathbf{I}^{skw} \\ \mathbf{E}_\omega &= \left[\frac{3}{5}E_{N\omega} - \frac{3}{5}E_{T\omega}^{sym}\right]\boldsymbol{I}_{vol} + \left[\frac{2}{5}E_{N\omega} + \frac{3}{5}E_{T\omega}^{sym}\right]\mathbf{I}^{sym} + E_{T\omega}^{skw}\,\mathbf{I}^{skw} \end{aligned} \tag{27}$$

The comparison of eq. (27) with the general isotropic non symmetric elastic tensors for decoupled membrane-bending behavior

$$\begin{aligned} \mathbf{E}_u &= \alpha_1\mathbf{I}_{vol} + [\alpha_2+\alpha_3]\mathbf{I}^{sym} + [\alpha_2-\alpha_3]\mathbf{I}^{skw} \\ \mathbf{E}_\omega &= \beta_1\mathbf{I}_{vol} + [\beta_2+\beta_3]\mathbf{I}^{sym} + [\beta_2-\beta_3]\mathbf{I}^{skw} \end{aligned} \tag{28}$$

then leads finally to the identifications

$$\begin{aligned} \alpha_1 &= \frac{3}{5}E_{Nu} - \frac{3}{5}E_{Tu}^{sym}; & \beta_1 &= \frac{3}{5}E_{N\omega} - \frac{3}{5}E_{T\omega}^{sym} \\ \alpha_2+\alpha_3 &= \frac{2}{5}E_{Nu} + \frac{3}{5}E_{Tu}^{sym}; & \beta_2+\beta_3 &= \frac{2}{5}E_{N\omega} + \frac{3}{5}E_{T\omega}^{sym} \\ \alpha_2-\alpha_3 &= E_{Tu}^{skw}; & \beta_2-\beta_3 &= E_{T\omega}^{skw} \end{aligned} \tag{29}$$

whereby $\alpha_1 := L$ and $\alpha_2+\alpha_3 := 2G$ are recognized as the common Lamé parameters, while $\alpha_2-\alpha_3 := 2G_c$ is the micropolar shear modulus which couples the skew-symmetric stress-strain components.

5.2 Micropolar Microplane Elastoplasticity

In this section the thermodynamically consistent formulation of the microplane-based micropolar elastoplastic model is presented both for the general case and for the von Mises type model.

5.2.1 General Case

The elastoplastic type of micropolar continuum response behavior is characterized by the additive decomposition of the macroscopic total strain and curvature tensors into elastic and plastic contributions

$$\begin{aligned} \boldsymbol{\epsilon} &= \boldsymbol{\epsilon}_e + \boldsymbol{\epsilon}_p \\ \boldsymbol{\kappa} &= \boldsymbol{\kappa}_e + \boldsymbol{\kappa}_p \end{aligned} \tag{30}$$

The kinematic constraint assumption extends the applicability of the additive decomposition to the microscopic level. As a consequence, the total strain and curvature components at microplanes can be expressed as

$$\begin{aligned} \epsilon_N^{sym} &= \epsilon_{N\,e}^{sym} + \epsilon_{N\,p}^{sym} & \kappa_N &= \kappa_{N\,e} + \kappa_{N\,p} \\ \boldsymbol{\epsilon}_T^{sym} &= \boldsymbol{\epsilon}_{T\,e}^{sym} + \boldsymbol{\epsilon}_{T\,p}^{sym} & \boldsymbol{\kappa}_T^{sym} &= \boldsymbol{\kappa}_{T\,e}^{sym} + \boldsymbol{\kappa}_{T\,p}^{sym} \\ \boldsymbol{\epsilon}_T^{skw} &= \boldsymbol{\epsilon}_{T\,e}^{skw} + \boldsymbol{\epsilon}_{T\,p}^{skw} & \boldsymbol{\kappa}_T^{skw} &= \boldsymbol{\kappa}_{T\,e}^{skw} + \boldsymbol{\kappa}_{T\,p}^{skw} \end{aligned} \tag{31}$$

In the most general case the tensor of internal variables includes the plastic contributions of all the strain and curvature components at the microplanes

$$\boldsymbol{q} = \boldsymbol{q}(\epsilon_{N\,p}^{sym}, \boldsymbol{\epsilon}_{T\,p}^{sym}, \boldsymbol{\epsilon}_{T\,p}^{skw}, \kappa_{N\,p}, \boldsymbol{\kappa}_{T\,p}^{sym}, \boldsymbol{\kappa}_{T\,p}^{skw}, \xi^{mic}) \tag{32}$$

whereby the scalar internal variable ξ^{mic} accounts for the simplest isotropic hardening/softening response.

The microscopic free energy follows from the definition of the elastic free energy and of the microscopic free energy functions in equations (17), (19) and (20) as

$$\begin{aligned} \psi^{mic} = {} & W_{N\,u}(\epsilon_N - \epsilon_{N\,p}) + W_{T\,u}^{sym}(\boldsymbol{\epsilon}_T^{sym} - \boldsymbol{\epsilon}_{T\,p}^{sym}) + W_{T\,u}^{skw}(\boldsymbol{\epsilon}_T^{skw} - \boldsymbol{\epsilon}_{T\,p}^{skw}) + \\ & W_{N\,\omega}(\kappa_N - \kappa_{N\,p}) + W_{T\,\omega}^{sym}(\boldsymbol{\kappa}_T^{sym} - \boldsymbol{\kappa}_{T\,p}^{sym}) + W_{T\,\omega}^{skw}(\boldsymbol{\kappa}_T^{skw} - \boldsymbol{\kappa}_{T\,p}^{skw}) + \\ & \int_0^{\xi^{mic}} \phi^{mic}(\tilde{\xi}^{mic}) d\tilde{\xi}^{mic} \end{aligned} \tag{33}$$

whereby the restricted format of isotropic hardening/softening behavior is taken into account by means of the term $\int_0^{\xi^{mic}} \phi^{mic}(\tilde{\xi}^{mic}) d\tilde{\xi}^{mic}$.

The constitutive stresses and couple stresses at microplanes are then obtained from the evaluation of the microscopic Clausius-Duhem inequality

$$\begin{aligned}
\sigma_N &= \frac{\partial \psi^{mic}}{\partial \epsilon_{N\,e}} = E_{N\,u}\,\epsilon_{N\,e} \qquad & \mu_N &= \frac{\partial \psi^{mic}}{\partial \kappa_{N\,e}} = E_{N\,\omega}\,\kappa_{N\,e} \\
\boldsymbol{\sigma}_T^{sym} &= \frac{\partial \psi^{mic}}{\partial \boldsymbol{\epsilon}_{T\,e}^{sym}} = \boldsymbol{E}_{T\,u}^{sym} \cdot \boldsymbol{\epsilon}_{T\,e}^{sym} \qquad & \boldsymbol{\mu}_T^{sym} &= \frac{\partial \psi^{mic}}{\partial \boldsymbol{\kappa}_{T\,e}^{sym}} = \boldsymbol{E}_{T\,\omega}^{sym} \cdot \boldsymbol{\kappa}_{T\,e}^{sym} \\
\boldsymbol{\sigma}_T^{skw} &= \frac{\partial \psi^{mic}}{\partial \boldsymbol{\epsilon}_{T\,e}^{skw}} = \boldsymbol{E}_{T\,u}^{skw} \cdot \boldsymbol{\epsilon}_{T\,e}^{skw} \qquad & \boldsymbol{\mu}_T^{skw} &= \frac{\partial \psi^{mic}}{\partial \boldsymbol{\kappa}_{T\,e}^{skw}} = \boldsymbol{E}_{T\,\omega}^{skw} \cdot \boldsymbol{\kappa}_{T\,e}^{skw}
\end{aligned} \tag{34}$$

The evolution of the internal variables is restricted by the inequality of the microscopic dissipation

$$\begin{aligned}
\mathcal{D}^{mic} \;=\; & \sigma_N\,\dot{\epsilon}_{N\,p} + \boldsymbol{\sigma}_T^{sym} \cdot \dot{\boldsymbol{\epsilon}}_{T\,p}^{sym} + \boldsymbol{\sigma}_T^{skw} \cdot \dot{\boldsymbol{\epsilon}}_{T\,p}^{skw} + \\
& \mu_N\,\dot{\kappa}_{N\,p} + \boldsymbol{\mu}_T^{sym} \cdot \dot{\boldsymbol{\kappa}}_{T\,p}^{sym} + \boldsymbol{\mu}_T^{skw} \cdot \dot{\boldsymbol{\kappa}}_{T\,p}^{skw} - \phi^{mic}\,\dot{\xi}^{mic} \geq 0
\end{aligned} \tag{35}$$

Thus, the yield function on each microplane can be defined in the form

$$\Phi^{mic} \;=\; \varphi(\sigma_N, \boldsymbol{\sigma}_T^{sym}, \boldsymbol{\sigma}_T^{skw}, \mu_N, \boldsymbol{\mu}_T^{sym}, \boldsymbol{\mu}_T^{skw}) - \phi^{mic}(\xi^{mic}) \leq 0 \tag{36}$$

whereby the function φ of the microscopic constitutive stresses and couple stresses is characterized by the gradients

$$\begin{aligned}
\nu_{N\,u} &\doteq \partial\varphi/\partial\sigma_N \quad & \boldsymbol{\nu}_{T\,u}^{sym} &\doteq \partial\varphi/\partial\boldsymbol{\sigma}_T^{sym} \quad & \boldsymbol{\nu}_{T\,u}^{skw} &\doteq \partial\varphi/\partial\boldsymbol{\sigma}_T^{skw} \\
\nu_{N\,\omega} &\doteq \partial\varphi/\partial\mu_N \quad & \boldsymbol{\nu}_{T\,\omega}^{sym} &\doteq \partial\varphi/\partial\boldsymbol{\mu}_T^{sym} \quad & \boldsymbol{\nu}_{T\,\omega}^{skw} &\doteq \partial\varphi/\partial\boldsymbol{\mu}_T^{skw}
\end{aligned} \tag{37}$$

For the associated case the plastic strain and curvature evolution laws are obtained from the variational problem defined by the dissipation inequality (36) under consideration of the convexity condition and of the constraint (36). For the general non-associated case we postulate instead

$$\begin{aligned}
\dot{\epsilon}_{N\,p} &= \dot{\gamma}^{mic}\,\vartheta_{N\,u} \qquad & \dot{\boldsymbol{\epsilon}}_{T\,p}^{sym} &= \dot{\gamma}^{mic}\,\boldsymbol{\vartheta}_{T\,u}^{sym} \qquad & \dot{\boldsymbol{\epsilon}}_{T\,p}^{skw} &= \dot{\gamma}^{mic}\,\boldsymbol{\vartheta}_{T\,u}^{skw} & \\
\dot{\kappa}_{N\,p} &= \dot{\gamma}^{mic}\,\vartheta_{N\,\omega} \qquad & \dot{\boldsymbol{\kappa}}_{T\,p}^{sym} &= \dot{\gamma}^{mic}\,\boldsymbol{\vartheta}_{T\,\omega}^{sym} \qquad & \dot{\boldsymbol{\kappa}}_{T\,p}^{skw} &= \dot{\gamma}^{mic}\,\boldsymbol{\vartheta}_{T\,\omega}^{skw} \qquad & \dot{\xi}^{mic} = \dot{\gamma}^{mic}
\end{aligned} \tag{38}$$

with the flow directions at each microplane

$$\begin{array}{llll} \vartheta_{N\,u} = \partial\breve{\Phi}/\partial\sigma_N & \boldsymbol{\vartheta}_{T\,u}^{sym} = \partial\breve{\Phi}/\partial\boldsymbol{\sigma}_T^{sym} & \boldsymbol{\vartheta}_{T\,u}^{skw} = \partial\breve{\Phi}/\partial\boldsymbol{\sigma}_T^{skw} \\ \vartheta_{N\,\omega} = \partial\breve{\Phi}/\partial\mu_N & \boldsymbol{\vartheta}_{T\,\omega}^{sym} = \partial\breve{\Phi}/\partial\boldsymbol{\mu}_T^{sym} & \boldsymbol{\vartheta}_{T\,\omega}^{skw} = \partial\breve{\Phi}/\partial\boldsymbol{\mu}_T^{skw} \end{array} \tag{39}$$

in terms of the plastic multiplier $\dot{\gamma}^{mic}$ and of the gradients to the microscopic plastic potentials $\breve{\Phi}$.

The Kuhn-Tucker loading-unloading conditions as well as the consistency condition can be defined on each microplane as

$$\Phi^{mic} \leq 0, \qquad \dot{\gamma}^{mic} \geq 0, \qquad \Phi^{mic}\,\dot{\gamma}^{mic} = 0, \qquad \dot{\Phi}^{mic}\,\dot{\gamma}^{mic} = 0 \tag{40}$$

An explicit solution for the plastic multiplier can be obtained from the consistency condition

$$\begin{array}{rcl} \dot{\gamma}^{mic} & = & \dfrac{1}{h}\left[\nu_{Nu}E_{Nu}\boldsymbol{N} + \boldsymbol{\nu}_{Tu}^{sym}\cdot\boldsymbol{E}_{Tu}^{sym}\cdot\boldsymbol{T}^{sym} - \boldsymbol{\nu}_{Tu}^{skw}\cdot\boldsymbol{E}_{Tu}^{skw}\cdot\boldsymbol{T}^{skw}\right] : \dot{\boldsymbol{\epsilon}} + \\ & & \dfrac{1}{h}\left[\nu_{N\omega}E_{N\omega}\boldsymbol{N} + \boldsymbol{\nu}_{T\omega}^{sym}\cdot\boldsymbol{E}_{T\omega}^{sym}\cdot\boldsymbol{T}^{sym} - \boldsymbol{\nu}_{T\omega}^{skw}\cdot\boldsymbol{E}_{T\omega}^{skw}\cdot\boldsymbol{T}^{skw}\right] : \dot{\boldsymbol{\kappa}} \end{array} \tag{41}$$

whereby

$$\begin{array}{rcl} h & = & \nu_{Nu}E_{Nu}\vartheta_{Nu} + \boldsymbol{\nu}_{Tu}^{sym}\cdot\boldsymbol{E}_{Tu}^{sym}\cdot\boldsymbol{\vartheta}_{Tu}^{sym} - \boldsymbol{\nu}_{Tu}^{skw}\cdot\boldsymbol{E}_{Tu}^{skw}\cdot\boldsymbol{\vartheta}_{Tu}^{skw} + \\ & & \nu_{N\omega}E_{N\omega}\vartheta_{N\omega} + \boldsymbol{\nu}_{T\omega}^{sym}\cdot\boldsymbol{E}_{T\omega}^{sym}\cdot\boldsymbol{\vartheta}_{T\omega}^{sym} - \boldsymbol{\nu}_{T\omega}^{skw}\cdot\boldsymbol{E}_{T\omega}^{skw}\cdot\boldsymbol{\vartheta}_{T\omega}^{skw} + H^{mic} \end{array} \tag{42}$$

and

$$H^{mic} = \frac{\partial\phi^{mic}(\xi^{mic})}{\partial\xi^{mic}} \tag{43}$$

Finally, the macroscopic elastoplastic constitutive equations can be expressed as

$$\begin{bmatrix} \dot{\boldsymbol{\sigma}}^t \\ \\ \dot{\boldsymbol{\mu}}^t \end{bmatrix} = \begin{bmatrix} \mathbf{E}_{ep}^{u,u} & \mathbf{E}_{ep}^{u,\omega} \\ \\ \mathbf{E}_{ep}^{\omega,u} & \mathbf{E}_{ep}^{\omega,\omega} \end{bmatrix} : \begin{bmatrix} \dot{\boldsymbol{\epsilon}} \\ \\ \dot{\boldsymbol{\kappa}} \end{bmatrix} \tag{44}$$

with the elastoplastic operators

$$\begin{aligned}
\mathbf{E}_{ep}^{u,u} &= \mathbf{E}_u - \frac{3}{2\pi}\int_\Omega \frac{1}{h}\tilde{\boldsymbol{n}}_u \otimes \tilde{\boldsymbol{m}}_u d\Omega \\
\mathbf{E}_{ep}^{\omega,\omega} &= \mathbf{E}_\omega - \frac{3}{2\pi}\int_\Omega \frac{1}{h}\tilde{\boldsymbol{n}}_\omega \otimes \tilde{\boldsymbol{m}}_\omega d\Omega \\
\mathbf{E}_{ep}^{u,\omega} &= -\frac{3}{2\pi}\int_\Omega \frac{1}{h}\tilde{\boldsymbol{n}}_u \otimes \tilde{\boldsymbol{m}}_\omega d\Omega \\
\mathbf{E}_{ep}^{\omega,u} &= -\frac{3}{2\pi}\int_\Omega \frac{1}{h}\tilde{\boldsymbol{n}}_\omega \otimes \tilde{\boldsymbol{m}}_u d\Omega
\end{aligned} \tag{45}$$

whereby the modified gradients are defined as

$$\begin{aligned}
\tilde{\boldsymbol{n}}_u &= E_{Nu}\nu_{Nu}\boldsymbol{N} + \boldsymbol{T}^{sym}\cdot[\boldsymbol{E}_{Tu}^{sym}\cdot\boldsymbol{\nu}_{Tu}^{sym}] - \boldsymbol{T}^{skw}\cdot[\boldsymbol{E}_{Tu}^{skw}\cdot\boldsymbol{\nu}_{Tu}^{skw}] \\
\tilde{\boldsymbol{m}}_u &= E_{Nu}\vartheta_{Nu}\boldsymbol{N} + \boldsymbol{T}^{sym}\cdot[\boldsymbol{E}_{Tu}^{sym}\cdot\boldsymbol{\vartheta}_{Tu}^{sym}] - \boldsymbol{T}^{skw}\cdot[\boldsymbol{E}_{Tu}^{skw}\cdot\boldsymbol{\vartheta}_{Tu}^{skw}] \\
\tilde{\boldsymbol{n}}_\omega &= E_{N\omega}\nu_{N\omega}\boldsymbol{N} + \boldsymbol{T}^{sym}\cdot[\boldsymbol{E}_{T\omega}^{sym}\cdot\boldsymbol{\nu}_{T\omega}^{sym}] - \boldsymbol{T}^{skw}\cdot[\boldsymbol{E}_{T\omega}^{skw}\cdot\boldsymbol{\nu}_{T\omega}^{skw}] \\
\tilde{\boldsymbol{m}}_\omega &= E_{N\omega}\vartheta_{N\omega}\boldsymbol{N} + \boldsymbol{T}^{sym}\cdot[\boldsymbol{E}_{T\omega}^{sym}\cdot\boldsymbol{\vartheta}_{T\omega}^{sym}] - \boldsymbol{T}^{skw}\cdot[\boldsymbol{E}_{T\omega}^{skw}\cdot\boldsymbol{\vartheta}_{T\omega}^{skw}]
\end{aligned} \tag{46}$$

Please note the resulting format of the micropolar microplane elastoplastic tangent operator is quite similar to that of the classical micropolar model (compare Willam et al. (1995) [22]) with exception of the integrals which account for the microscopic contribution to the macroscopic operator in case of the micropolar microplane formulation.

5.2.2 von Mises Type Model

The classical micropolar elastoplastic von Mises type model, see e.g. de Borst (1991) [12], is characterized by the yield condition

$$\Phi^{mac} = \sqrt{3J_2} - \phi^{mac} = 0 \qquad J_2 = \frac{1}{4}\boldsymbol{s}:\boldsymbol{s} + \frac{1}{4}\boldsymbol{s}:\boldsymbol{s}^t + \frac{1}{2l_c^2}\boldsymbol{\mu}:\boldsymbol{\mu} \tag{47}$$

with $\boldsymbol{s}$ the deviator of $\boldsymbol{\sigma}$ and with yield stress with linear hardening

$$\phi^{mac} = \phi_0^{mac} + H^{mac}\zeta^{mac} \tag{48}$$

Here the evolution of the hardening/softening parameter is given by

$$\dot{\xi}^{mac} = \sqrt{\frac{1}{3}\dot{\boldsymbol{\epsilon}}_p:\dot{\boldsymbol{\epsilon}}_p + \frac{1}{3}\dot{\boldsymbol{\epsilon}}_p:\dot{\boldsymbol{\epsilon}}_p^t + \frac{2}{3}l_c^2\dot{\boldsymbol{\kappa}}_p:\dot{\boldsymbol{\kappa}}_p} = \dot{\gamma}^{mac} \tag{49}$$

Assuming that the second invariant of the stress deviator tensor $\boldsymbol{s}$ is a function of the tangential stress vectors and of the tangential couple stress vectors of the microplanes, the von Mises yield condition at the microplane level can be expressed in the format

$$\Phi^{mic} = \sqrt{\boldsymbol{\sigma}_T^{sym} \cdot \boldsymbol{\sigma}_T^{sym} + \boldsymbol{\sigma}_T^{skw} \cdot \boldsymbol{\sigma}_T^{skw} + \frac{1}{l_c^2}[\boldsymbol{\mu}_T^{sym} \cdot \boldsymbol{\mu}_T^{sym} + \boldsymbol{\mu}_T^{skw} \cdot \boldsymbol{\mu}_T^{skw}]} - \phi^{mic} \leq 0 \qquad (50)$$

with the yield stress with linear hardening

$$\phi^{mic} = \phi_0^{mic} + H^{mic}\xi^{mic} \qquad (51)$$

Here the evolution of the hardening/softening parameter is given by

$$\dot{\xi}^{mic} = \sqrt{\dot{\boldsymbol{\epsilon}}_{Tp}^{sym} \cdot \dot{\boldsymbol{\epsilon}}_{Tp}^{sym} + \dot{\boldsymbol{\epsilon}}_{Tp}^{skw} \cdot \dot{\boldsymbol{\epsilon}}_{Tp}^{skw} + l_c^2[\dot{\boldsymbol{\kappa}}_{Tp}^{sym} \cdot \dot{\boldsymbol{\kappa}}_{Tp}^{sym} + \dot{\boldsymbol{\kappa}}_{Tp}^{skw} \cdot \dot{\boldsymbol{\kappa}}_{Tp}^{skw}]} = \dot{\gamma}^{mic} \qquad (52)$$

which, similarly to the macroscopic description, coincides with the plastic multiplier.

6 LOCALIZATION CONDITIONS

In the continuum approach the localization condition is associated with a discontinuity or jump across a singularity surface S of second order. Assuming that the surface with the direction N separates the continuum $\mathcal{B}$ into two regions $\mathcal{B}^+$ and $\mathcal{B}^-$ which are connected by the jumps in the underlying gradient fields across this surface. In Cosserat-continua weak jumps across a singularity surface may occur not only in the strain field, but also in the field of micro-curvatures. Departing from the notion of a continuous solid in which the velocity and rotation rate fields are initially continuous and where discontinuities of their spacial derivatives develop across the singular surface, we arrive to the first localization condition by means of the Cauchy lemma relating the traction rate vector and the stress tensor, the elastoplastic constitutive relation and the Maxwell theorem, in the form

$$\begin{bmatrix} \boldsymbol{Q}_L^{u,u} & \boldsymbol{Q}_L^{u,\omega} \\ \boldsymbol{Q}_L^{\omega,u} & \boldsymbol{Q}_L^{\omega,\omega} \end{bmatrix} \cdot \begin{bmatrix} \dot{\gamma}^u \boldsymbol{M}^u \\ \dot{\gamma}^\omega \boldsymbol{M}^\omega \end{bmatrix} = \begin{bmatrix} \boldsymbol{O} \\ \boldsymbol{O} \end{bmatrix} \qquad (53)$$

with the suboperators

$$Q_{ij}^{\eta\psi} = N_k \, E_{kilj}^{\eta\psi} \, N_l \quad \text{where} \quad \eta, \psi u, \omega. \qquad (54)$$

To satisfy (53), the localization operator Q_L must be singular. Thus, the determinant must be zero:

$$\det(\boldsymbol{Q}_L) = \det \begin{bmatrix} \boldsymbol{Q}_L^{u,u} & \boldsymbol{Q}_L^{u,\omega} \\ \boldsymbol{Q}_L^{\omega,u} & \boldsymbol{Q}_L^{\omega,\omega} \end{bmatrix} = O \qquad (55)$$

in case of discontinuous bifurcation.

The second localization condition follows from the balance of linear and angular momenta on both sides of the singularity surface. Particularly, the consideration of the

bifurcated stress and couple stress in the angular momentum equation lead to the condition

$$\boldsymbol{e} : [[\dot{\boldsymbol{\sigma}}]] = 0 \tag{56}$$

This second condition has to be fulfilled simustaneously with the first condition to admit discontinuous bifurcation.

Both localization conditions are analyzed in the present research work for the micropolar microplane model and for the classical micropolar model. The predictions of these localization conditions obtained with both models are compared.

7 NUMERICAL ANALYSIS

In this section we analyze the predictions of the micropolar microplane elastoplastic von Mises model for the uniaxial tensile and simple shear tests. Figure 2 illustrates the boundary conditions of these tests which were analyzed under plane strain constraints. In both one element meshes of Figure 2 the standard bilinear quadrilateral finite element with four integraion points was used. This finite element formulation of micropolar continuum problems is obtained by means of discretizations of the weak form of the balance equations in the spirit of the Dirichlet variational principle, see Willam et al. (1995). Thereby the displacements and rotations (and their variations) are approximated by the same shape functions according to the Galerkin-Bubnov method.

In the simple shear test, full displacement and rotation restraint were considered on the nodes located on the bottom of the quadrilateral element while only the vertical displacements were restrained on the other element nodes. On the other hand, in case of the axial extension test, the full displacement and rotation restraint were assumed only in one element node as indicated in Figure 2 while in other two nodes one displacement possibility together with the in plane rotation were restrained according to the double symmetry of the problem. Both, the yield condition and hardening/softening evolution law are those indicated in section 7.2. The micropolar elastic parameters at microplanes for the numerical analysis were $E = 30000\, N/mm^2$, $\nu = 0.2$, $G_c = G$ and $l_c = 1mm$. Consequently the other parameters resulted: $E_{Nu} = 33333.33$, $G = 12500$, $E_{Tu}^{sym} = 19444.45$, $E_{Tu}^{skw} = 25000$, $E_{N\omega} = E_{T\omega}^{sym} = E_{T\omega}^{skw} = 25000$.

The microscopic and macroscopic von Mises stresses ϕ_0^{mic} and ϕ_0^{mac}, respectively, were chosen so that similar predictions of the J_2 type maximum strength corresponding to both the uniaxial tensile and simple shear tests are obtained with the microscopic and the macroscopic micropolar models. So, the resulting values were $\phi_0^{mic} = 23.5\ N/mm^2$ and $\phi_0^{mac} = 50.0\ N/mm^2$ for the axial extension test while these stresses are $\phi_0^{mic} = 29.0\ N/mm^2$ and $\phi_0^{mac} = 50.0\ N/mm^2$ for the simple shear test.

7.1 Axial Tension Test

Figure 3 illustrates the numerical predictions of the uniaxial tensile test with the micropolar microplane elastoplastic model and with the classical micropolar elastoplastic model.

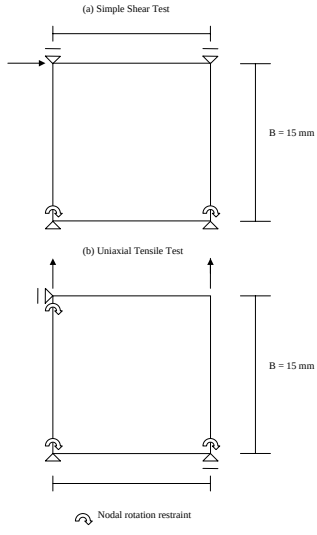

Figure 2: Boundary conditions of the plane strain uniaxial tensile and simple shear tests

Three different types of evolution laws of the stress functions ϕ^{mic} and ϕ^{mac} were considered for these models, corresponding to perfect plasticity, linear hardening and linear softening behavior.

The first observation from the comparison between the predictions of both types of micropolar models is that their response behaviors during the elastic range agree very well. Also the overall predictions of both models in the plastic range under linear softening and perfect plasticity are very similar. However, under linear hardening assumption the classical microplane model leads to a much more ductil response behavior indicating that this formulation is more sensitive to variations of the hardening evolution law.

We analyze now the fundamental differences between the numerical predictions of the micropolar microplane and of the classical micropolar model with perfect plasticity in Figure 3. In the case of the classical micropolar model with perfect plasticity the requirement for constant values of J_2 due to the yield condition

$$\Phi^{mac} = \sqrt{3J_2} - \phi_0^{mac} = 0$$

is responsible for the plateau in the J_2 evolution which immediately follows the elastic response, as indicated in Figure 4. On the other hand, the evolution of the the axial tensile force as well as that of the vertical tensile stress in Figures 3 and 4, respectively, show a smooth transition from the elastic to the perfect plastic regime.

The micropolar microplane model with perfect plasticity leads to a macroscopic stress tensor's evolution during the axial extension test characterized by an initial smooth soft-

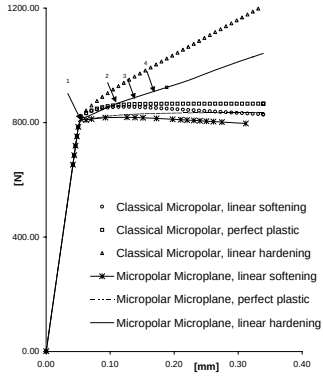

Figure 3: Load-displacement predictions. Axial extension test.

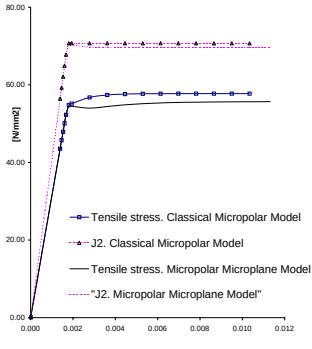

Figure 4: Stress-strain predictions. Axial extension test.

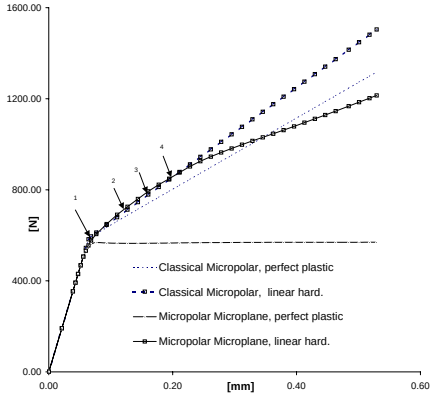

Figure 5: Load-displacement predictions. Simple shear test.

ening response of J_2 and subsequent plateau. The same response behavior are observed in the evolutions of the vertical tensile stress in Figure 4 and of the axial force in Figure 3.

7.2 Simple Shear Test

The numerical predictions of the micropolar microplane model for the simple shear test and the comparison with the corresponding predictions of the classical micropolar model are indicated in Figure 5. Both a linear hardening and a perfect plastic evolution laws were assumed for ϕ^{mic} and ϕ^{mac} in equations (48) and (51), corresponding to the microplane model and to the macroscopic model, respectively. It is important to note that in the simple shear test, contrarily to the axial extension test, the microrotations are activated. The results in Figure 5 also indicate that the micropolar microplane model with perfect plasticity leads, as expected, to a plateau of the external shear force. However, this is not the case of the predictions corresponding to the classical micropolar model which leads to continuus hardening of the external shear force although perfect plasiticity was considered. This is due to the evolution of the nonuniform microrotations which are activated during this test.

8 CONCLUSIONS

In this work the thermodynamically consistent elastic and inelastic micropolar formulations by Etse, Nieto and Steinmann (2002) were analyzed. Thereby, the main assumption is the incorporation of a microscopic free Helmholtz energy on every microplane, which in the present case includes the contributions of the additional degree of freedom and stiffness of the micropolar continuum, represented by the micro rotations and the couple stresses. Also an uncoupled format of the free energy in terms of the membrane and bending contributions is included.

The solutions for the micropolar microplane elastoplastic model include the macroscopic explicit formulation of the constitutive tangential moduli in terms of the microscopic contributions. The general elastoplastic formulation for the micropolar microplane model was particularized for von Mises type elastoplasticity.

The numerical results in this work show the predictions of the J_2 elastoplastic model for the uniaxial tensile and simple shear tests. Also the main differences with the corresponding predictions of the classical micropolar elastoplastic model were highlighted.

The results demonstrate that micropolar microplane constitutive theory allows the formulation of material models based on relevant aspects of the microstructure of engineering materials which exceeds the capacity of the classical macroscopic model theories.

The analysis of the localization indicator which belongs to the scope of work of the present research program is being developed. The corresponding results will be illustrated in the oral presentation of this work.

REFERENCES

[1] Batdorf, S.B. & B. Budiansky [1949]. "A mathematical theory of plasticity based on the concept of slip." Technical Note 1871. *National Advisory Committee for Aeronautics (NACA), Washington, D.C.*

[2] Bazant, Z.P. [1984]. "Imbricate Continuum and its Variational Derivation." *J. Eng. Mech.*, 110, pp. 1693-1712.

[3] Bazant, Z.P. & P.G. Gambarova [1984]. "Crack shear in concrete: Crack band microplane model." *J. Struct. Eng.*, ASCE, 110, pp. 2015-2036.

[4] Bazant, Z.P. & B.H. Oh [1985]. "Microplane model for progressive fracture of concrete and rock." *J. Eng. Mech.*, 111, pp. 559-582.

[5] Bazant, Z.P. & B.H. Oh [1986]. "Efficient numerical integration on the surface of a sphere." *ZAMM*, 66(1), pp. 37-49.

[6] Bazant, Z.P. & P. Prat [1988]. "Microplane model for brittle plastic material: Part I - Theory, Part II - Verification." *J. Eng. Mech.*, 114, pp. 1672-1702.

[7] Carol, I., Z.P. Bazant & P. Prat [1991]. "Geometric damage tensor based on microplane model." *J. Eng. Mechanics*, 117, pp. 2429-2448.

[8] Carol, I., Z.P. Bazant & P. Prat [1992]. "New explicit microplane model for concrete: Theoretical aspects and numerical implementation." *Int. J. Solids & Structures*, 29,

pp. 1173-1191.

[9] Carol, I. & Z.P. Bazant [1997]. "Damage and plasticity in microplane theory." *Int. J. Solids & Structures*, 34, pp. 3807-3835.

[10] Carol, I., M. Jirasek & Z.P. Bazant [2001]. "A thermodynamically consistent approach to microplane theory. Part I: Free energy and consistent microplane stresses." *Int. J. Solids & Structures*, 38, pp. 2921-2931.

[11] Cosserat, E. & F. Cosserat [1909]. "Theory des corps deformables." *Herman et fils*, Paris.

[12] de Borst, R. [1991]. "Simulation of strain localization: A reappraisal of the Cosserat Continuum." *Engg. Comp.*, Vol. 8, pp. 317-332.

[13] Eringen, A.C. [1968]. "Theory of Micropolar Elasticity." *Fracture, an Advanced Treatise*. Ed. L. Liebowitz, Academic Press, New York.

[14] Etse, G., M. Nieto & P. Steinmann [2002]. "A Micropolar Microplane Theory." *Fracture, an Advanced Treatise*. Ed. L. Submitted to *Int. J. Eng. Sci.*

[15] Kuhl, E., Steinmann. P. & I. Carol [2001]. "A thermodynamically consistent approach to microplane theory. Part II: Dissipation and inelastic constitutivr modeling" *Int. J. Solids & Structures*, 38, pp. 2933-2952.

[16] Lubarda, V. & D. Krajcinovic [1993]. "Damage Tensors and the Crack Density Distribution." *Int. J. Solids & Structures*, 30, pp. 2859-2877.

[17] Mühlhaus, H-B. [1989]. "Application of Cosserat theory in numerical solutions of limit load problems." *Ing. Archive*, Vol. 59, pp. 124-137.

[18] Sluys, P. [1992]. *Wave propagation, localization and dispersion in softening solids*. Dissertation, Delft University of Tech., Delft.

[19] Steinmann, P., K. Willam [1991]. "Localization within the framework of micropolar elastoplasticity." *60th Anniv. Volume Prof. Lippmann*, V. Mannl, O. Brueller and J. Najar (eds.), Springer Verlag Berlin, pp. 296-313.

[20] Taylor, G. I. [1938]. "Plastic strain in metals." *J. Inst. Metals*, 62, pp. 307-324.

[21] Willam, K. & A. Dietsche [1992]. "Regularization of localized failure computations." In Proc. of *Int. Conf. Computational Plasticity, COMPLAS III*. Edt. E. Onate, E. Hinton and R. Owen, Pineridge Press Swansea, pp. 2185-2204.

[22] Willam, K., A. Dietsche, M-M. Iordache & P. Steinmann [1995]. "Localization in Micropolar Continua." *Continuum Models for Materials with Microstructure*. Ed. H-B. Mühlhaus. J.Wiley & Sons Ltd., pp. 297-339.